A PROPOSAL FOR AN INTENSE CYCLOTRON-BASED THERMAL NEUTRON SOURCE

S. Tazawa
Sumitomo Heavy Industries, Ltd., Toyo-shi, 799-13 Japan

and

W.L. Whittemore
General Atomics, San Diego, California 92138, U.S.A.

ABSTRACT

A cyclotron-based thermal neutron source using the Be(p,n) reaction is summarized, with particular regard to basic parameters affecting source intensity and characteristics such as bombarding energy, current, moderation of fast neutrons and thermal neutron flux, based mainly on the experimental results from an existing cyclotron of proton energy 18 MeV. The thermal neutron flux intensity is estimated based on the commercially available high intensity current from an H^- cyclotron and compared with common neutron sources including nuclear reactors. Also, amplification of these thermal neutrons using U-235 bundles is estimated.

1. INTRODUCTION

One of the practical applications of neutrons is N-ray radiography, which is a non-destructive tool used to detect the presence and/or structural nature of materials opaque to neutrons. This technique is similar to X-ray radiography in that radiation is passed through an object being inspected and an image is recorded on photographic film or through real-time imaging on such memory devices as magnetic tape, floppy disks or laser disks.

Neutron radiography differs from X-ray radiography in that, unlike X-rays, which are increasingly absorbed by materials of increasing atomic number, neutrons are absorbed selectively by various elements depending on the characteristics of the nucleus.

As a result, neutrons of the correct energy, unlike X-rays, can penetrate heavy metals like steel and lead and be scattered by hydrogen-bearing materials like plastics or absorbed by specific elements like Gd, Cd, of Boron. This technique was initially developed using highly intense thermal neutron fluxes obtained from a nuclear reactor. Its applicability has been tested in aviation, defense and nuclear industries for pyrotechnic components, composite material, nuclear spent fuel and corrosion detection of airplane wings (Table 1).

Table 1. Example of Neutron Radiography

	Film Method
Pyrotechnics	: Detonating cord, igniter plug, fusing device
Composite Materials	: ERP, FRM, Honeycomb Structure
Turbine Engine	: Residual core detection of turbine blade
Electrical Components	: Electrical contact point, potting of resin
Ceramics	: Green body
Nuclear fuel	: Spent fuel detection
	R-T Imaging
Aluminum Structure	: Corrosion and moisture detection in wing
Flow visualization	: Plastic extruder, Heated water
Two phase flow	NH_3 in heat pipe, Freon in refrigerator
& Streak line	Streak line of Pb-Bi eutectic metal

2. CHARACTERISTICS OF A CYCLOTRON-BASED NEUTRON RADIOGRAPHY (NR) SYSTEM

Cyclotron-based neutron sources are not only used for fast neutron therapy, but also as practical thermal neutron sources for NR. An actual cyclotron system is routinely operational at Toyo Works[1)] of SHI for charged particle activation analysis (CPAA) of light elements like B, C, N and O, thin layer activation (TLA) for machine wear measurement with joint collaboration of KfK, and irradiation for power transistor and switching devices like GTOs, IGBTs, power diodes and thyristors. The basic principle of a cyclotron-based neutron radiography system is to bombard a beryllium target with a proton beam of 18 MeV at a current of 50 μA, producing fast neutrons of 3.4 MeV through the ^{9}Be(p,n)^{9}B reaction.[2)]

A special feature of this cyclotron-based system is that it can produce a much larger fast neutron yield than the ordinary rather low energy electrostatic accelerator systems like a Van de Graaff system[3)] using ^{9}Be(d,n)^{10}B reaction with an energy range of a few MeV, or a tritium neutron generator using T(d,n)^{4}He with a 100 kV range.

This situation is shown in Fig. 1 which presents the relation between fast neutron yield and bombarding energy specially for the compact cyclotron energy region with Be(p,n) and Be(d,n). Much more needs to be said here about the various energies of fast neutrons from these accelerators and the ability to moderate them, as the neutron energy of most interest is in the thermal region of 0.025 eV, in order to obtain good contrast in the radiograph images. Also, most elements have a maximum scattering cross section which serves to enhance the contrast for different elements in the actual object.

Thermalisation is achieved in this system by elastic and inelastic scattering processes with hydrogen atoms contained in the moderator, which in this system is constituted from polyethylene. This moderation process is similar to that in a nuclear reactor, but the small size of the neutron source requires special consideration. The thermalized neutrons are extracted from the moderator with some beams lacking definition, which causes poor edge definition due to penumbral shadow. The neutron current is required to be nearly parallel for use with thick specimens. The neutrons are collimated by passing them through a divergent type of collimator characterized by L/D where L is the length and D the entrance diameter of the collimator.

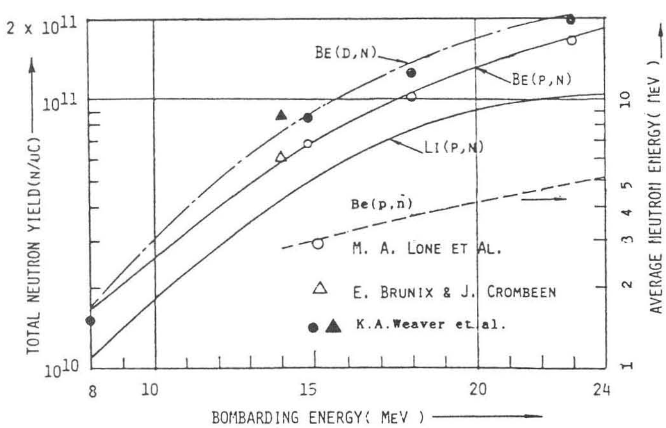

Fig. 1. Fast neutron yield from thick Be and Li targets bombarded by protons and deuterons versus average energy for Be(p,n).

When one requires a small penumbral shadow, its width is related to the height of the object (h) by Eq. 1:

$$w = h/(L/D) \quad (1)$$

Larger L/D is realized at the sacrifice of the neutron flux current (J), which is shown generally to vary as the inverse square of L/D (Eq. 2).

$$J/J_i = 1/16(L/D)^2 \quad (2)$$

Then the use of a collimator with large L/D requires long exposure time and is not practical in actual operation. So, optimization for good images and shorter exposure times is very important for the design of the system. The neutrons incident on the object and passing through it, impinge on a converter screen and are converted to another form of radiation such as photons for a fluorescent converter or electrons for a Gd film converter, which then exposes a silver halide film. Usually it requires a large fluence for the Gd converter, plasma sputtered on an aluminum film, but excellent image quality can be obtained. With a small neutron beam current, a long exposure is usually required. Fluorescent converters like LiF-ZnS,[4] activated with Ag or GdO_2S (Tb) are mostly used for real-time imaging coupled with a nocturnal TV camera. In Fig. 2 the sensitivity of various types of converter is shown using a film exposure method for the film density versus the neutron fluence.

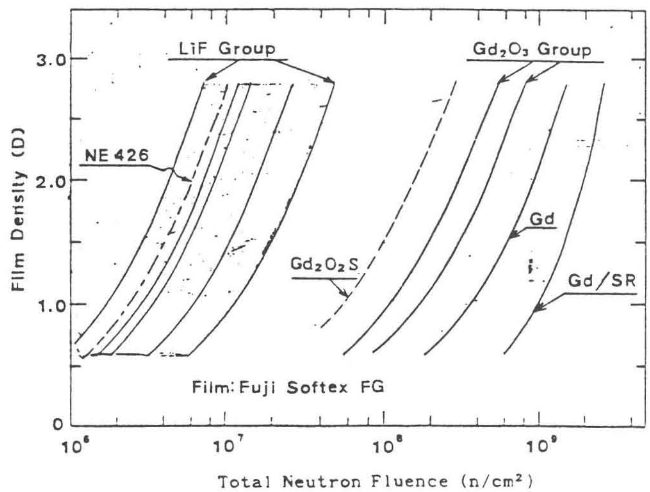

Fig. 2. Sensitivity of several neutron converters using either the Li(n,α) or the Gd(n,γ) reaction emitting 70 keV internal conversion electrons.

Table 2. Characteristics of the Cyclotron-based NR Facility at SHI

Cyclotron	: Model 370
Particle & Energy	: proton 18 MeV, deuteron 10 MeV, ^{3}He 24 MeV
Current(max)	: 50 μA
Nuclear Reaction	: ^{9}Be(p,n)^{9}B
Moderator	: High density polyethylene at inside
Dimension	: 700 mm cube(400 mm cube)
Collimator	: Borated polyethylene(B_2O_3:10%)
Extraction	: Downward and horizontal direction
L/D	: 32, 44(32), 74 , Field size : 14" x 17"
Neutron flux at L/D = 44	: Horizontal 1.7×10^6, Vertical 1.0×10^6 n/cm^2/sec
Cd ratio	: 4.2 n/γ ratio : 1.5 x 10^5 n/cm^2/mR
Neutron Component by ASTM 545-81 Beam Purity Indicator	
Thermal neutron content(%)	: 65.3 (48.1), Horizontal(Vertical)
Scatter " (%)	: 0.5 (8.1)
γ ray content (%)	: 3.7 (1.3)
Pair creation (%)	: 3.2 (1.9)

*( ) is obtained from the umbra shadow method of ASTM E803-81.
*Film : Kodak SR with 25 μ Gd converter

2.1. Cyclotron-based Neutron Radiography Facility

A typical example of a cyclotron-based neutron radiography facility is shown in Fig. 3. In this facility two neutron radiography ports are provided for efficient beam utilization. The neutron beams emerging from the target are directed mostly forward so that vertical beams are collected from the beams directed downwards from the stochastic collisions of the thermalisation process. Therefore the vertical beam port provides more thermal neutrons than the horizontal port. In practice, handling the object material is more convenient for the vertical port, as the objects are simply placed on a film cassette.

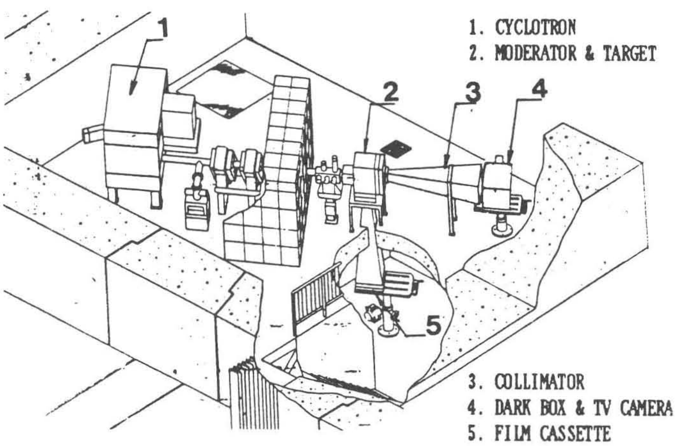

Fig. 3. NR Facility at Toyo Works of SHI.

2.2. Thermal Neutron Enhancement in the Moderation Process

The typical flux obtained is shown in Table 3, where we compare several cases of our improvements to the moderation process by decreasing the target diameter from ϕ120 mm to 60 mm and changing the moderator material from normal to high density polyethylene, where the hydrogen content was 8.0 and 8.3 $\times 10^{22}$ per cc. The smaller target space contributes a large flux increase of 110% and the use of high density polyethylene gives 36%, resulting in an overall improvement by a factor 2.8; but vertical extraction is 62% of horizontal extraction and further improvement is necessary.

Table 3. Thermal Neutron Flux Ratios (%) for $L/D = 44$

Collimator End Direction	Horizontal	Vertical
High/Normal Polyethylene	136%	120%
Target ϕ60/120 mm	210%	145%

Also, this targetry and moderator system was initially tested with 17 MeV and 30 MeV protons at Tohoku University.[5] The thermalization efficiency for each system is compared where the thermalization factor is defined as the ratio of source yield (neutrons/sec) to the peak thermal flux (neutron /cm^2.s) in a given moderator. A typical example[6] gives a value of 40 for Be(p,n) with 2.8 MeV protons and 300 for Be(d,n) with 2.8 MeV deuterons, as summarized in Table 4.

Table 4. Example of Thermalisation Factor for Be(p,n) and Be(d,n)

Energy (MeV)	Source S_0(n/μC)	Thermalisation Factor	Remarks: Target diameter + Materials
p 3.2	10^{11}	40	M.R.Hawkesworth[6]
d 3.2		300	"
p 17	0.93×10^{11}	~940	ϕ120+Normal Poly.
p 18	1.06×10^{11}	1040	"
"	"	1040	"
"	"	880	"
"	"	660	ϕ60+Normal Poly.
"	"	590	ϕ60+High Density Poly.
p 30	3.26	~990	ϕ120+N

3. THE IMAGING SYSTEM AND ITS QUALITY

For real-time imaging the neutron radiography image is converted to a TV signal and digital imaging processing can then be used for construction of the final image. One example of imaging is shown in Fig. 4a and 4b, where a single TV frame with a real time of 1/30 second, and its image integration over 256 frames, are presented, respectively.

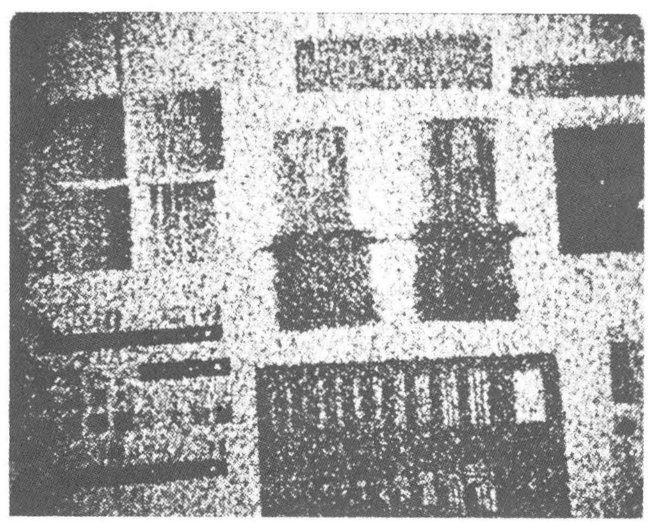

Fig. 4a. One TV frame image of real-time neutron radiograph of turbine blade at neutron flux of 1.1×10^6n/cm^2/sec, with LiF-ZnS converter (A4 Kasei Opto. Inc.) and SIT TV camera (Tokyo Electric Co.) with RCA 4804 SIT tube.

From Fig. 4a the neutron radiographic image looks as if it is composed from dot points and requires great neutron flux density for noise suppression; actually, as shown in Fig. 4b, with 256 frames of image integration, a digital image of 512 $\times$ 512 pixels can be achieved with 8-bit gray levels. A single pixel corresponds to 0.38 $\times$ 0.33 mm^2 in Fig. 4. If the neutron flux is 10^6 n/cm^2/sec, one pixel receives only 42 neutrons for one NTSC system frame of 33 msec. Statistical analysis of the gray level for a definite domain of pixels showed that the noise appearing in the raw image of Fig. 4a can be explained well by neutron fluctuations due to Poisson statistics.[7] If one integrates 256 frames, the fluctuation decreases to 1% as shown in Fig. 4b, corresponding approximately to 8×10^6 n/cm^2 fluence. This value gives a film density of 3 in Fig. 2 for the fluence versus film density curve for the LiF-ZnS converter that was used for this R-T imaging. Here we can conclude that 10^7n/cm^2 fluence is a criterion for obtaining good neutron radiography images, but images with a few 10^6 n/cm^2 fluence level can be reconstructed by digital local filtering techniques like median, contrast stretching, fast Fourier method etc.

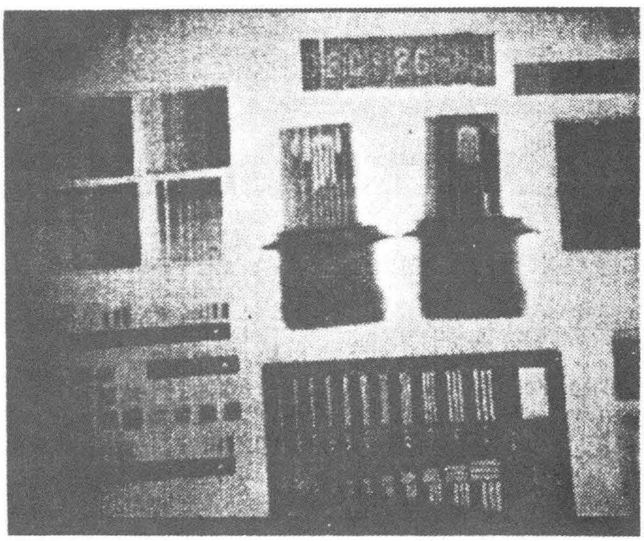

Fig. 4b. Image integration of 256 frames of Fig 4a.

4. NEUTRON RADIOGRAPHY EXAMPLE

We have conducted many real-time imaging experiments on flow visualization as shown in Table 1. One of the real-time NR applications is the visualization of streak lines in liquid metal, as used for the coolants of highly dense heat sources like fast fusion reactors, nuclear fusion reactors, etc. Here we applied real-time NR imaging for visualization of Pb-Bi eutectic metal using a Cd-Au tracer and a Cd dye method. This eutectic metal target is considered as one of the candidates for a neutron spallation target where the cooling is designed to occur by natural convective flow.[8,9] As this target is intended for use with a highly intense 1 mA beam of 590 MeV protons, any turbulence or dead space in the flow may be crucial for the cooling. Observation of the streak line is difficult except by NR, as light and X-rays are not opaque for the metal. A neutron radiograph of the Cd-Au tracer is shown in Fig. 5a, where we made a forced flow of the Pb-Bi, melted at 125°C, from the upper of wall (left) to the center of the hill, in a two-dimensional model of the target, simulating the convective flow of the actual target, where the beams hit the bottom from the down to the up direction. The tracer is prepared with 82.6% gold content to be the same density as the Pb-Bi (10.5) with a shape of few mm length. The arrow lines show the tracers of Au-Cd. Figure 5b shows the streak-lines drawn by tracing the video-tapes of every movement of the tracers by the use of two gray levels of image processing.

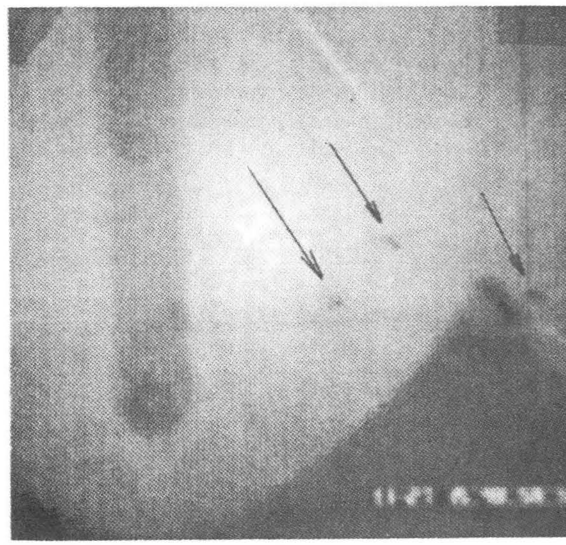

Fig. 5a. Visualization of tracers of Au_3Cd in liquid Pb-Bi eutectic metal.

5. CONCLUSION AND FURTHER POSSIBILITY FOR AN ACCELERATOR SOURCE

We have described a cyclotron-based thermal neutron source using the (p,n) reaction on a beryllium target, together with some examples of NR imaging. H^- cyclotrons have been recognized for their production of high-current proton beams up to the 1 mA level while maintaining stable operation. For efficient moderation of fast neutrons the energy of an H^- cyclotron should be in the 22 MeV energy range. Here we simply extend our 18 MeV cyclotron-based source to 22 MeV by estimating the target yield from Fig. 1 and assuming the same thermalization factor of 600 as at 18 MeV (Table 4). If we can design a target resisting 22 kW heat loss, the thermal neutron flux will reach that from a small reactor – 5×10^6n/cm^2/sec with a L/D=100 collimator. Also, the neutron flux with a subcritical multiplier, fueled with U-235, gave a multiplication factor of five in the previous study.[1] If we use this multiplier for the cyclotron source, the thermal neutron fluxes are at the same level or exceed those from the TRIGA reactor. The conceptual arrangement of the target, moderator and the uranium bundles is shown in Fig. 6. We summarize these results in Table 5 for comparison with another type of intense neutron source.

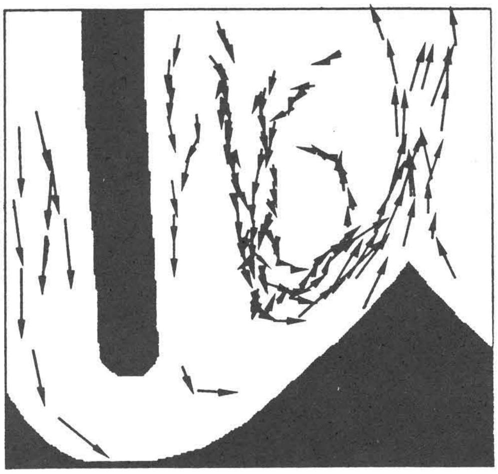

Fig. 5b. Streak lines drawn by movement tracers of Au_3Cd in Pb-Bi eutectic metal in a forced flow from the left of the upper wall to the center of the target.

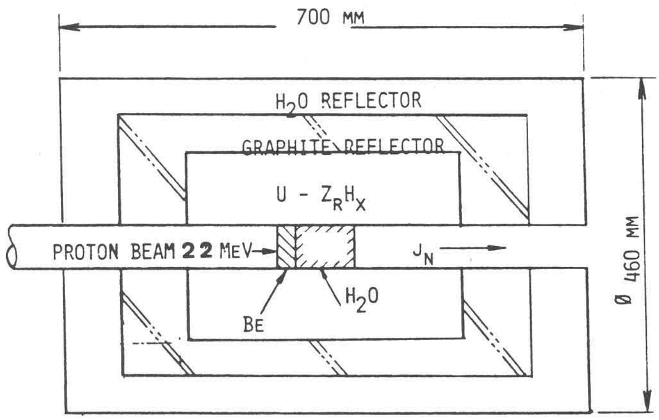

Fig. 6. Concept of amplification of neutrons using uranium bundles and a target.

Table 5. Comparison of typical thermal neutron source

Source	Characteristics	L/D	Source Flux (n/sec)	Output Flux (n/cm^2/sec)	Remarks
D-T Sealed Tube	225 kV	12	4×10^{11}	2.5×10^5	10)
RFQ Linac	p 3.9 MeV, 1 mA	24	1.3×10^{12}	3×10^6	AccSys Catalog
Van de Graaff	d 3MeV, 300 μA	30	2.6×10^9	3×10^5	3)
TRIGA Reactor	250 kW	100	10^{13} (n/cm^2/sec)	1×10^7	
Cyclotron	p 18 MeV, 50 μA	32	5.3×10^{12}	1.7×10^6	H^+ extraction
	p 22 MeV, 1 MA	100	1.6×10^{14}	5×10^6	H^- "
	"	100	" "	2×10^7	U multiplier 2)*

*Assuming a factor five multiplication with water moderator, presuming the normal polyethylene and water are equivalent for thermalization factor.

6. ACKNOWLEDGEMENT

We appreciate Prof. A. Ono, Dr. N. Takenaka, Dr. K. Sonoda of Kobe Univ. group for R-T imaging and the analysis. We would thank Dr. Y. Takeda of PSI for suggesting the liquid metal visualization and offering the model targets.

7. REFERENCES

1) S. Tazawa and T. Nakanii, "Present status of the cyclotron-based neutron radiography" **Proc. 3rd WCNR** (Kluwer, Osaka, 1989) pp.213-220.
2) S. Tazawa and W.L. Whittemore, "Thermal neutron intensity in cyclotron-based neutron radiography systems" *ibid.*, pp.221-229.
3) Jin-Si Kwon and W.L. Whittemore, **Proc. 2nd WCNR** (Reidel, Paris, 1986) pp.231.
4) Y. Suzuki, E. Hiraoka, S. Tazawa *et al.*, "Development of imaging converter", **Proc. 3rd WCNR** (Kluwer, Osaka, 1989) pp.277-279.
5) S. Tazawa and T. Nakanii *et al.*, "Cyclotron-based neutron radiography cacility", **Proc. 2nd WCNR** (Reidel, Paris, 1986) pp.231-238.
6) M.R. Hawkesworth, Atomic Energy Rev. **15**, No.2, pp.169 (1977).
7) R. Taniguchi, A. Ono, S. Tazawa *et al.*, "Statistical properties of R-T neutron radiography image", **Proc. 2nd WCNR** (Reidel, Paris, 1986) pp.555-562.
8) N. Takenaka, A. Ono, S. Tazawa *et al.*, "Visualization of streak lines in liquid metal by neutron radiography", presented at the 4th WCNR, San Francisco, May 10-14, 1992.
9) F. Atchison, W.E. Fischer, M. Pepin and Y. Takeda, "Spallation neutron source", **Proc. on Neutron Scattering in the 'Nineties** (IAEA, Jülich, 1985) pp.171-177.
10) S. Cluzeau *et al.*, "Thermal neutron source using a neutron sealed tube", presented at the 4th WCNR, San Francisco, May 10-14, 1992.